Deanonymizing Mobility Traces: Using Social Networks as a Side-Channel

Mudhakar Srivatsa
IBM T.J. Watson Research Center
msrivats@us.ibm.com

Mike Hicks
University of Maryland
mwh@cs.umd.edu

ABSTRACT

Location-based services, which employ data from smartphones, vehicles, etc., are growing in popularity. To reduce the threat that shared location data poses to a user's privacy, some services anonymize or obfuscate this data. In this paper, we show these methods can be effectively defeated: a set of location traces can be deanonymized given an easily obtained social network graph. The key idea of our approach is that a user may be identified by those she meets: a *contact graph* identifying meetings between anonymized users in a set of traces can be structurally correlated with a social network graph, thereby identifying anonymized users. We demonstrate the effectiveness of our approach using three real world datasets: University of St Andrews mobility trace and social network (27 nodes each), SmallBlue contact trace and Facebook social network (125 nodes), and Infocom 2006 bluetooth contact traces and conference attendees' DBLP social network (78 nodes). Our experiments show that 80% of users are identified precisely, while only 8% are identified incorrectly, with the remainder mapped to a small set of users.

Categories and Subject Descriptors

C.2.0 [**General**]: Security and protection

General Terms

Security, Management

Keywords

Information Flow, Graph Deanonymization, Spatio-temporal Data

1. INTRODUCTION

Applications that employ sensor data (e.g., location, acceleration) generated by everyday mobile devices such as smartphones, tablets, and cars have become quite popular [3, 11, 15, 21, 32]. As examples, CarTel [15] collects location information from GPS sensors in cars to infer traffic conditions, and GreenGPS [11] computes fuel-optimal routes from OBD-II sensors installed in cars. Human mobility patterns have been used for urban planning and traffic forecasting [13]. While useful, these services pose a risk: a user's mobility trace, if revealed, can provide information about habits, interests and activities—or anomalies to them—which in turn may exploited for illicit gain via theft, blackmail, or even physical violence [2].

To reduce the risk of exposing too much information, it has been suggested that those who collect mobility traces could *anonymize* them by removing personally identifying information (PII), such as name, address, or birthday. Unfortunately, prior work has shown that PII removed from other kinds of datasets can be recovered by employing *auxiliary information* [24]; this recovery process is called *deanonymization*. The key question is: in the case of mobility traces does there exist readily available auxiliary information with which an adversary could effectively perform deanonymization? In this paper, we show that the answer is 'yes.'

Mobility traces can be deanonymized by exploiting the *social network* of the participating users. Such social networks are readily available: friend relationships can be found from public Facebook data, co-authorship relationships from DBLP, and business relationships from LinkedIn. The key insight is that a pattern of meetings between users suggests they have relationship; this relationship may be mirrored in their social network and thus the social network can be used to recover PII removed from a trace.

The key idea behind our approach is to identify *discriminating features* in the social network graph when performing deanonymization. To illustrate what we mean, consider the simplified example in Figure 1. Let us consider four users, b, c, d, and e, and their respective anonymized user identities b', c', d' and e'. Suppose that we have deanonymized users $b' = b$ and $c' = c$ (e.g., they are the landmark nodes). In this example, we observe that the following feature can be used to discriminate d and e: d is a friend of *both* b and c, whereas e is a friend of *only* b. Let $f(b)$ denote the set of b's friends in the social network; then the following constraints hold $d \in f(b) \cap f(c)$ and $e \in f(b) \setminus f(c)$. One can now transfer these constraints to the contact graph as equations over variables v_d and v_e (the nodes in the contact graph that potentially maps to node d and node e in the social network) and require that $v_d \in f(b') \cap f(c')$ and $v_e \in f(b') \setminus f(c')$ (for notational simplicity, f is overloaded to operate on both the social network and the contacts graph). In this example, solving for the variables v_d and v_e results in an unique solution, namely, $v_d = d'$ and $v_e = e'$. On the other hand if both d' and e' exhibited identical contact patterns with b' and c', we will not be able to discriminate user d from user e. Hence, both the mappings $\{d = d'$ and $e = e'\}$ and $\{d = e'$ and $e = d'\}$ would seem equally likely from the point of view of the deanonymization algorithm.

We validate our approach using three real world datasets: Uni-

CCS'12, October 16–18, 2012, Raleigh, North Carolina, USA.
Copyright 2012 ACM 978-1-4503-1651-4/12/10 ...$15.00.

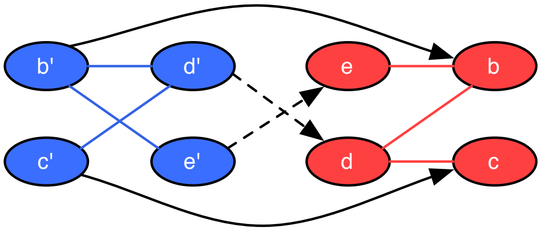

Figure 1: Deanonymization requires Discriminative Features: the Contact Graph is on the left, the Social Network on the right

	St Andrews	Smallblue	Infocom06
Comm network type	WiFi	IM	Bluetooth
No comm nodes	27	125	78
Duration (days)	30	30	4
Granularity (secs)	300	300	120
No contacts	18,241	240,665	182,951
Social network type	Facebook	Facebook	DBLP
No social nodes	27	400	616

Figure 2: Datasets

versity of St Andrews mobility traces and social network (27 nodes each), SmallBlue contact traces and Facebook social network (125 nodes), and Infocom 2006 bluetooth contact traces and conference attendee's DBLP social network (78 nodes). Our initial results show that our approach deanonymizes 80% of the nodes in the traces correctly, 8% incorrectly, and the remaining 8% it is able to correctly map a node to a small set of users (no more than three), one of which is the correct one.[1] Our results also show that even when about 25% of the social network and the contact graph is intentionally modified (e.g., edges/nodes are added/removed) our approach is effective; further, when a small fraction (5%) of select node mappings (in particular, nodes with low centrality score) are known a priori, then the effectiveness of our approach can exceed 95% (i.e., 95% of nodes are correctly mapped).

The next section sets up the problem more formally and describes our evaluation datasets. Section 3 presents our approach in detail and evaluates it on these datasets. Section 4 evaluates the impact on deanonymization of adding noise to the data and of using inaccurate or incomplete social network graphs. Section 5 discusses related work, and Section 6 concludes.

2. PROBLEM SETUP

2.1 Notation and Terminology

V_S denotes the set of users with each user having a unique identifier. L denotes the set of location identifiers with each location having a unique identifier. $d(l_1, l_2)$ denotes the distance between two locations l_1 and l_2 in L. We write A to denote a location trace of the form $\langle u, l, t\rangle^*$, where $u \in V_S$, $l \in L$ and t is a timestamp.

Similarity Measure	St Andrews	Smallblue	Infocom06
Graph edit distance / Num edges	8 / 62	28 / 375	22 / 212
Common sub-graph / Num nodes	18 / 27	72 / 125	42 /78

Figure 3: Graph Similarity Measures

V_C denotes the set of anonymized user identifiers, i.e., the mapping between the set of users V_S and V_C is unknown. L' denotes the set of obfuscated location identifiers. We remark the location identifiers may be obfuscated using several techniques including the addition of random noise or generalization (i.e., reducing the granularity of location information). For instance, a location l in L may be perturbed to locations l'_1 and l'_2 in L' with probability p and $(1-p)$ respectively for some $0 \leq p \leq 1$ (random noise); or two locations l_1 and l_2 in L may be mapped to the same location l' in L' (generalization). We remark that the efficacy of deanonymization degrades with the extent of location obfuscation.

A' denotes an anonymized location trace of the form $\langle u', l', t\rangle^*$, where $u' \in V_C, l' \in L'$ and t is a time stamp. The goal of deanonymization is to infer the mapping between the set of users in V_S and V_C. As discussed earlier, the technique used for deanonymization depends on the nature of available auxiliary information. In this paper we consider auxiliary information that is represented by a social network $S = (V_S, E_S)$, where an edge in set E_S has the form $\langle u_1$, u_2, r_{12}, $w_{12}\rangle$ such that u_1, $u_2 \in V_S$ (note that users in the social network correspond to non-anonymous user identifiers), $r_{12} \in R$ an directed relationship between users u_1 and u_2 and R is a finite set of relationship types (e.g., manager, friend, colleague, co-author, etc.). In addition to relationship type we consider two types of annotations w_{12} to the social network links: one that corresponds to the strength of a relationship denoted by a weight between [0, 1] (e.g., normalized number of co-authored papers) and second that corresponds to periodicity at which a relationship is active (e.g., *colleague* relationship is active every day from 9am-5pm).

In order to structurally match (and de-anonymize) a mobility trace against a social network we construct a contact graph C. Intuitively a contact graph captures pair-wise meetings between two users. Given two events $\langle u'_1$, l'_1, $t_1\rangle$ and $\langle u'_2$, l'_2, $t_2\rangle$ in an anonymized location trace, we say that there is a contact between users u_1 and u_2 if $d(l'_1, l'_2) \leq \tau_1$ and $|t_1 - t_2| \leq \tau_2$, for some thresholds τ_1, $\tau_2 \geq 0$. Given a sequence of contacts between two users u'_1 and u'_2 we apply Fourier transform to detect periodicity in such contacts. We construct contact graphs at different time granularities – based on the most dominant periodicity of contacts derived by applying the Fourier transform. The contact graph C thus generated is of the form $C = (V_C, E_C)$, where the edges in E_C are of the form $\langle u'_1$, u'_2, c_{12}, $w_{12}\rangle$ and the class type c_{12} is obtained by manual classifying contacts based on the time-of-the-day and w_{12} denotes the frequency of contacts within the period of interest.

2.2 Datasets

In this section we briefly review the datasets that were used in our study. A description of these datasets [4, 1, 28] is shown in Figure 2. The St Andrews university dataset captures the WiFi hotspot (within the university) to which a user (a student volunteer) is connected at intervals of 300 seconds. We assume that two users are in contact if they are both connected to the same WiFi hotspot for an interval of time that spans 600 seconds. The contact graph includes a weight – the frequency of inter-user contacts over the duration of the trace. The St Andrews dataset also includes a social network (gathered from Facebook) on the same set of student volunteers. The social network has 0/1 link weights based on two users being a *friend* on the Facebook social network. We note that in our datasets the ground truth, that is, the mapping between nodes in the social network and the contact graph is given to us.

The Smallblue dataset captures contacts between users using an instant messenger on an enterprise network. Two users are said to be contact if they exchange chat messages back and forth with each other. A session of such chat messages between a pair of users

[1] Nodes in the remaining 4% are correctly mapped to a set of four or more users

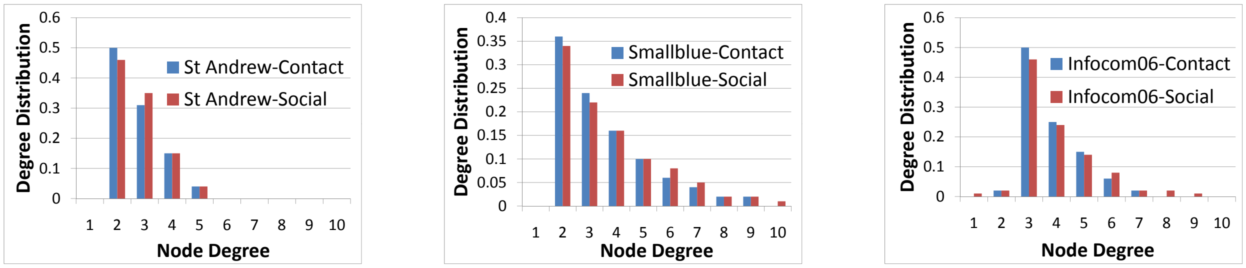

Figure 4: Degree Distribution: St Andrews, Smallblue and Infocom06

constitutes one contact. The contact graph is constructed in a similar manner with link weights that correspond to the frequency of inter-user contacts over the duration of the trace. In addition to the mobility trace the dataset also includes a social network (gathered from Facebook) on a superset of users. The social network has 0/1 link weights based on two users being a *friend* on the Facebook social network.

The Infocom06 dataset is a Bluetooth contact trace of Infocom 2006 conference attendees that volunteered to contribute their mobility information. When two users are within Bluetooth connectivity range (typically less than 10 meters), a Bluetooth connection is established between the user devices. If such a connection lasts for 600 seconds we assume that the users are in contact with each other (we ignored contacts during session breaks and lunch breaks). In addition the dataset also includes a list of 616 attendees (names and affiliations) of Infocom 2006. The volunteers (78 of them) are a strict subset of the conference attendees. We use DBLP (co-authorship database [9]) to construct a social network over the conference attendees − the social network has 0-1 link weights based on the normalized number of co-authored papers between two users: if P_{u_1} and P_{u_2} denote the set of papers that includes user u_1 and u_2 on the author list then the weight of the link between the users is given by $\frac{|P_{u_1} \cap P_{u_2}|}{|P_{u_1} \cup P_{u_2}|}$.

2.3 Structural Similarity

The key hypothesis of our approach is that the social network and the contact graph bear structural similarities. We show that this is indeed the case using three well accepted measures of graph similarity: graph edit distance (minimum number of edges that need to be added and/or deleted for an exact match), maximum common sub-graph (number of vertices in the largest common sub-graph) and node degree distribution. We remark that the graph edit distance measure typically applies to graphs that have identical number of vertices, while the latter measures do not impose such a restriction. In order to simplify the measurement of such graph similarity measures we round-off edge weights in the social network and the contact graph to either 0 or 1.

Figure 3 shows graph similarity measures using the graph edit distance and the maximum common sub-graph measures. Figure 4 shows the degree distributions of the contact graph and the social network using the datasets. These figures show that the contact graph and the social network tend to bear a lot of similarity; in our datasets, the average ratio of graph edit distance to the number of edges is about 10.3% (lower the better), the average ratio maximum common sub-graph to the number of nodes is about 60% (higher the better), the average Kullback and Leibler (KL) symmetrised divergence measure [31] between the node degree distributions is about 0.062 bits (lower the better).

3. GRAPH DE-ANONYMIZATION

We examine a two step solution to match the contact graph against the social network. In the first step we bootstrap the matching problem by exploiting inherent heterogeneity in the graphs to identify landmark nodes. In the second step we extend a mapping between landmark nodes to all the nodes in the graph by identifying discriminating features in the original graph. We explore three techniques for this second step. In the remainder of this section we describe our algorithm in detail and evaluate each of the techniques using the previously described datasets. Results were computed on an Intel i5 quad-core processor operating at 2.4 GHz with 4 GB RAM running RedHat Enterprise Linux 5.4.

3.1 Initial Landmarks Selection

For the first step, we identify landmark nodes using a node centrality measure [25, 7], which is a measure of the relative importance of a vertex within a graph. Centrality is very well studied metric in both graph theory and social network analysis, e.g., to determine how important a person is within a social network or how well-used a road is within an urban network. We identify landmark nodes as those with high centrality metric. Past work [12] has shown that node centrality in contact graphs and social networks generally follows a heavy tailed distribution; hence, there are a small number of nodes (outliers) with a high centrality score, while a vast majority of the nodes belong to the tail of the distribution. Therefore we identify the top k central nodes, for $k \ll |V_C|$, $|V_S|$, in both the contact graph and the social network as landmark nodes; we experimentally show that for small values of k the set of top-k centrality nodes in both the social network and the contact graph are likely to be the same. Further, given k landmark nodes in both the contact graph and the social network there are at most $k!$ mappings between them. Since k is typically small even a brute force enumeration of all possible mappings is feasible.

While there are several measures of centrality, in this paper we adopt the *node betweeness* metric. The betweenness centrality measure (as applied to a static graph) for node n is a normalized measure over the number of all-pair shortest paths in a graph that includes node n. In general, if a large number of shortest paths pass through node n, then node n has a higher betweeness centrality measure. We use this betweeness measure for centrality computation in the static social network

For the contract graph we observe that in a contact graph a 'path' exists over time. Hence, the standard shortest path based definition of node betweeness does not directly apply to the contact graph. Hence, we develop a novel centrality measure that applies to contact graphs. First, we recognize that a path between two nodes A and B in the contact graph is via a sequence of contacts N_1, N_2, $\cdots$, N_{r-1}. Hence, we adopt the following definition of paths in contact graph:

DEFINITION 1. **Opportunistic path** [12]

A r-hop opportunistic path P_{AB} =(V_P, E_P) between nodes A and B consists of a node set $V_P = \{A, N_1, N_2, \cdots, N_{r-1}, B\} \subset V$ and an edge set $E_P = \{\langle A, N_1, w_1\rangle, \langle N_1, N_2, w_2\rangle, \cdots, \langle N_{r-1}, B, w_r\rangle\} \subset E$ such that $N_i \neq N_j$ for any $1 \leq i < j \leq r-1$. The path weight is the probability $p_{AB}(T)$ that A may reach B along P_{AB} within time T.

We model the inter-contact time X_k between nodes N_k and N_{k+1}, as a random variable with a probability density function (PDF) $p_{X_k}(x)$. In our datasets we observed that $p_{X_k}(x)$ was exponentially distributed: $p_{X_k}(x) = w_k e^{-w_k x}$. However, we remark that the approach is applicable to any arbitrary distribution. Assuming that $p_{X_k}(x)$ is exponentially distributed, $Y = \sum_{k=1}^{r} X_k$ following a hypoexponential distribution [27], such that

$$p_Y(x) = \sum_{k=1}^{r} G_k^{(r)} p_{X_k}(x), \qquad (1)$$

where the coefficients $G_k^{(r)} = \prod_{s=1, s\neq k}^{r} \frac{w_s}{w_s - w_k}$.

From Eq. (1), the path weight is written as

$$p_{AB}(T) = \int_0^T p_Y(x)dx = \sum_{k=1}^{r} G_k^{(r)} \cdot (1 - e^{-w_k T}), \qquad (2)$$

The centrality metric C_i for a node i is then defined as follows:

$$C_i = \frac{1}{N-1} \cdot \sum_{j=1, j\neq i}^{N} p_{ij}(T), \qquad (3)$$

where N is the total number of nodes in the network. Intuitively, this metric is a measure of distance from a randomly chosen node in the network to node i. Due to the heterogeneity of the pairwise contact frequency in different traces, different values of T were adaptively chosen; T is set as 1 hour for the Infocom traces, 6 hours for the St Andrews and Smallblue traces.

Figures 5 and 6 shows the centrality scores of nodes in the contact graph and the social network respectively. We observe due to the inherent heterogeneity of these graphs, only a few select nodes have high centrality scores. More interestingly, we observe that the same of set of nodes that have high centrality score in the contact graph also has a high centrality score in the social network. Indeed we note that the set of top-k nodes (ordered by centrality score) is identical for both the contact graph and the social network. For e.g., node identifiers 1, 7 and 18 in the St Andrews dataset are the top 3 central nodes in both the contact graph and the social network; node identifiers 8, 25, 41, 55, 100 and 119 are the top 6 central nodes in the both the contact graph and the social network in the Smallblue dataset; node identifiers 8, 24, 34, 47 and 72 are the top 5 central nodes in the both the contact graph and the social network in the Infocom06 dataset.

Note that at this stage we still do not have a mapping between the landmark nodes; however, given k landmark nodes there are at most k! mappings. In the subsequent sections we propose techniques to start with a mapping of landmark nodes and de-anonymize the rest of the contact graph. We repeat this exercise for all such k! mappings between the landmark nodes; using a goodness-of-fit test on the thus derived mappings we select the most likely mapping between the nodes in the contact graph and the social network.

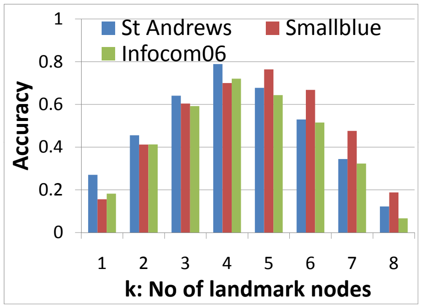

(a) Accuracy

k	St Andrews	Smallblue	Infocom06
1	1.9	195	47
2	2	196	47.4
4	2.2	198	48
8	2.4	200	49

(b) Computation times (seconds)

Figure 7: Distance Vector Results

Given a possible mapping between such landmarks, the next step is to use various graph features to deduce mappings for other nodes. Formally, $L_C = \{c_1, \cdots, c_k\}$ and $L_S = \{s_1, \cdots, s_k\}$ denote the landmark nodes in the contact graph and the social network respectively, and the initial mapping is $c_i = s_i$ for all $1 \leq i \leq k$. Given this initial mapping, we consider three possible techniques—distance vectors, spanning tree matching, and local sub-graph features—detailed in the next three subsections.

3.2 Distance Vector

The first technique we consider is to map nodes that have similar *distance vectors*. For each non-landmark node in the contact graph and the social network, its distance vector contains distances between the node to the k landmark nodes. Hence, for a node n, its distance vector is given by $\{d_{n1}, \cdots, d_{nk}\}$, where d_{ni} denotes the distance from node n to landmark i (i.e., c_i in the contact graph and s_i in the social network).

Given two nodes c in the contact graph and s in the social network we quantify a mapping score as $w_{cs} = -\sqrt{\sum_{i=1}^{k} (d_{ci} - d_{si})^2}$. Now we construct a bipartite graph with vertex set $(V_C \setminus L_C) \cup (V_S \setminus L_S)$, where V_C and V_S are the set of vertices in the contact graph and the social network respectively; for every node $c \in V_C \setminus L_C$ and $s \in V_S \setminus L_S$ we add an edge between node c and node s with weight w_{cs}. Now the node mapping problem reduces to a *maximum weighted bipartite graph matching problem* that determines matching pairs of vertices in $V_C \setminus L_C$ and $V_S \setminus L_S$ respectively. We use the Hungarian algorithm [6] that solves the weighted graph matching problem in bipartite graphs in $O(|V|^3)$, where V is the set of vertices and E is the set of edges in the bipartite graph. The result of this algorithm is pairs of matched nodes $s' \in V_C \setminus L_C$ and $s \in V_S \setminus L_S$. We denote the overall matching score as $\sum_{s \in V_S \setminus L_S} w_{s's}$. We repeat this procedure for all k! mappings between landmark nodes and finally select the mapping that results in the highest matching score.

Figure 7(a) shows the accuracy of de-anonymization as we vary k. We observe that initially as k increases the accuracy of de-

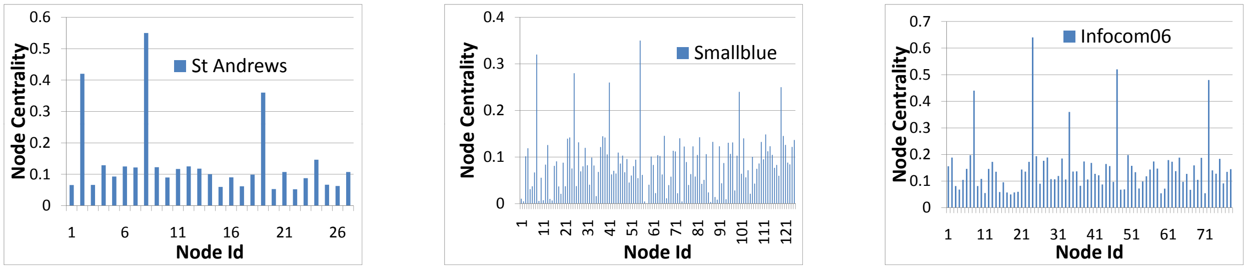

Figure 5: Node Centrality in Contact Graph: St Andrews, Smallblue and Infocom06

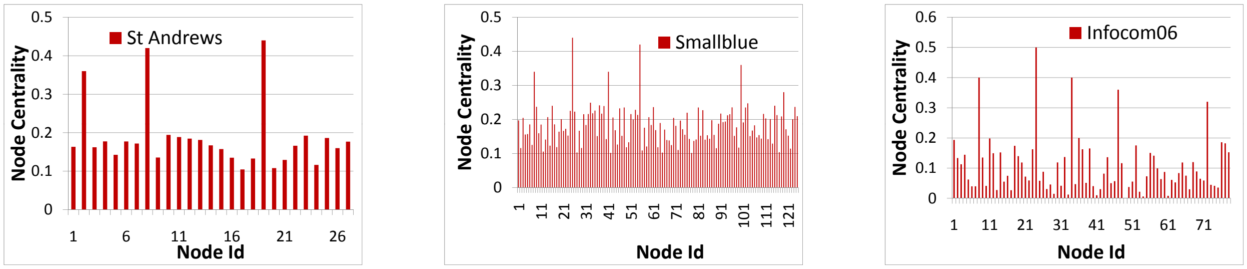

Figure 6: Node Centrality in Social Network: St Andrews, Smallblue and Infocom06. Notice that the peaks (high centrality nodes) in the contact graph (Figure 5) and the social network (Figure 6) match.

anonymization process improves — since larger number of landmarks improves the precision of node distance vectors. However, as k increases further the set of landmark nodes in the contact graph and the social network are no longer identical; hence, the overall efficacy of node mapping decreases.

Figure 7(b) shows the computation cost of deriving node mappings given a mapping for landmark nodes. We note that given a landmark mapping the computation cost does not increase significantly with k — the number of landmark nodes. As k increases we need to compute distances from more landmark nodes to all the other nodes in both the contact graph and the social network. This operation costs $O(k|E|)$. Once such distances are computed the cost of computing similarity is $O(k|V|^2)$. However, the cost of the weighted bipartite graph matching $O(|V|^3)$ which dominates the computation cost is independent of k. Note that Figure 7 shows the cost for a given landmark node mapping — hence, the overall computation cost has to be scaled with $k!$ (for every possible landmark node mapping). We observe that on the 125 node Smallblue dataset with k = 5 nodes the total time to de-anonymize is 5!*200 seconds or about 6.7 hours.

3.3 Randomized Spanning Trees

An obvious approach to performing the mapping would be to compute general graph isomorphism between the contact and social network graphs. However, general graph isomorphism is an NP-hard problem, so this approach would be computationally intractable for large contact graphs and social networks. We observe that a classical approach to derive mappings between entities in a high dimensional space is to project them to a lower dimensional space wherein it may be easier to identify such mappings. Following this observation, we significantly lower the complexity of the graph mapping by reducing it to randomized tree mapping problem, for which poly-time algorithms exist [29].

In this solution we project both the contact graph C and the social network S into randomized spanning trees. We note given any graph G the number of spanning trees of graph G is given by Kirchhoff's theorem [14]: $\frac{1}{|V|} * \Pi_{i=1}^{|V|-1} \lambda_i$, where λ_i are the non-zero eigenvalues of G's Laplacian matrix. The Laplacian matrix Q of a graph G is defined as $Q = D - A$, where D is a diagonal matrix with the i^{th} diagonal element set to the degree of node i and A is the adjacency matrix of graph G (i.e., the ij^{th} element in A is 1 if there exists an edge between node i and j; 0 otherwise). Kirchhoff's theorem also allows us to explicitly enumerate all spanning trees of a graph and thus enables us to select a random set of such spanning trees.

Given two such spanning trees C_T and S_T we seed the mappings between landmark nodes and then apply a classical tree-to-tree editing algorithm [29] to derive node mappings between other nodes in the tree. The runtime complexity of the tree-to-tree editing algorithm is $O(|V_C||V_S|)$. We quantify the efficacy of a mapping using the graph edit distance between the labeled contact graph and the social network. Over multiple such randomized spanning trees and all $k!$ landmark node mappings we select the mapping that has the least edit distance between the labeled contact graph and the social network.

Figure 8(a) shows the accuracy of de-anonymization as we increase the number of randomized spanning trees (with the number of landmark nodes k set to 4) constructed from the contact graph and the social network. The figure also shows the accuracy of de-anonymization as we increase the number of landmark nodes (with the number of randomized spanning trees set to 128). The figure indicates that the accuracy of de-anonymization can be as large as 72%, 80% and 68% respectively for St Andrews, Smallblue and Infocom06 datasets.

Figure 8(b) shows the tree mapping for a given pair of span-

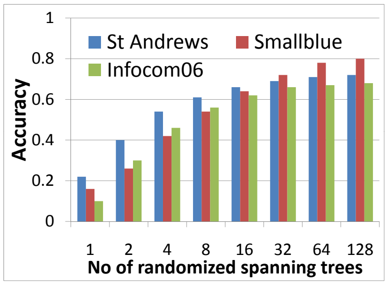

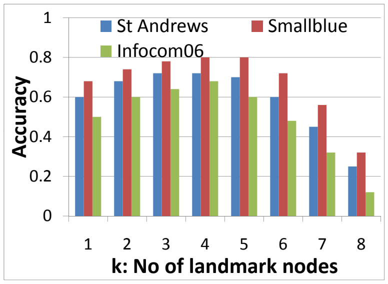

(a) Accuracy

k	St Andrews	Smallblue	Infocom06
1	0.12	2.98	1.08
2	0.13	3.29	1.17
4	0.14	3.51	1.26
8	0.16	4.02	1.44

(b) Computation times (seconds)

Figure 8: Randomized Spanning Tree Results

ning trees C_T and S_T. We observe that on the 125 node Smallblue dataset with k = 5 nodes and 128 randomized spanning trees, the total time to de-anonymize is 5!*128*4.02 seconds or about 6.2 hours.

3.4 Recursive Sub-Graph Matching

For our final technique, we propose to use sub-graph features to derive mappings between the contact graph and the social network. We start with the seed set of landmark nodes and recursively expand such mappings to other nodes in the contact graph. The key idea is to model the node mapping as a constraint satisfaction problem (CSP) [22]. We leverage the social network to derive constraints on node mappings as follows. For each node a in the social network we create a variable x_a in the CSP. We constrain all variables x_a to take values from the set V_C, where V_C denotes vertices in the contact graph. If there is a link between users a and b in the social network we introduce conjunctive constraints of the form: $x_a \in f(x_b)$ and $x_b \in f(x_a)$, where $f(x_a)$ denotes the set of edges incident on node x_a in the contact graph. Indeed since the contact graph and the social network may not have an exact mapping the CSP may have no feasible solutions. Hence, we solve for MAX-CSP that minimizes the number of constraint violations (i.e., minimizes the number of unsatisfied constraints).

In general solving such a MAX-CSP is a NP-hard problem. Instead we solve a *dynamic* CSP problem that only introduces constraints of the form $x_a \in f(x_b)$ such that value of x_b has already been determined — the dynamic CSP is bootstrapped using landmark node mappings, i.e., the value of x_{l_i} is assumed to be known for every landmark node l_i. We use a CSP solver in ILOG [16] to recursively expand the set of node mappings from the landmark nodes to span all the nodes in the contact graph. The CSP solver exploits a combination of backtracking (e.g., to undo incorrect node mappings), constraint propagation and local search to optimally solve the dynamic MAX-CSP problem. Further, the CSP solver exploits the absence of cyclical dependences in our constraints (note that we introduce a constraints $x_a \in f(x_b)$ only when the value of x_b is known) to scalably solve the node mapping problem.

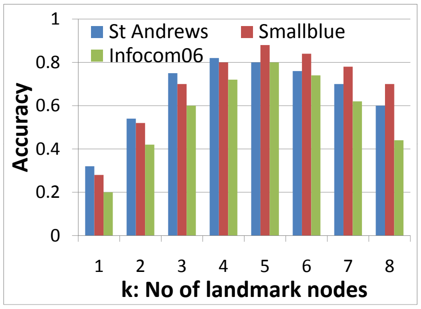

(a) Accuracy

k	St Andrews	Smallblue	Infocom06
1	0.70	12.60	5.25
2	0.72	12.96	5.42
4	0.76	13.68	5.75
8	0.84	15.12	6.36

(b) Computation times (seconds)

Figure 9: Recursive Sub-Graph Matching Results

dataset	$\log_2 \lvert aut(C) \rvert$	$\log_2 \lvert aut(S) \rvert$	$\log_2 \lvert V \rvert !$
St Andrews	7.7	7.9	93
Smallblue	18.2	18.4	696
Infocom06	16.5	18.6	382

Figure 10: Number of Automorphisms

Figure 9(a) shows the accuracy of de-anonymization as we increase the number of landmark nodes. The figure indicates that the accuracy of de-anonymization can be as large as 82%, 88% and 80% respectively for St Andrews, Smallblue and Infocom06 datasets. Figure 8(b) shows the time taken to solve the dynamic MAX-CSP problem for a given landmark node mapping. We observe that on the 125 node Smallblue dataset with k = 5 nodes, the total time to de-anonymize is 5!*15.12 seconds or about 0.5 hours. We note that the computational complexity of recursive sub-graph matching using the dynamic CSP approach (without backtracking) is $O(|V| * max\_node\_degree)$. With limited backtracking (say, at most b local backtrackings) the complexity is still pseudo-polynomial in $|V|$: $O(|V| * max\_node\_degree^b)$.

3.5 Optimality: Graph Automorphism Bound

In this section we present solutions to analyze the efficacy of graph de-anonymization. First, we make a simple observation that efficacy of node mapping is fundamentally limited by number of graph *automorphisms*. Automorphism of a graph is a form of sym-

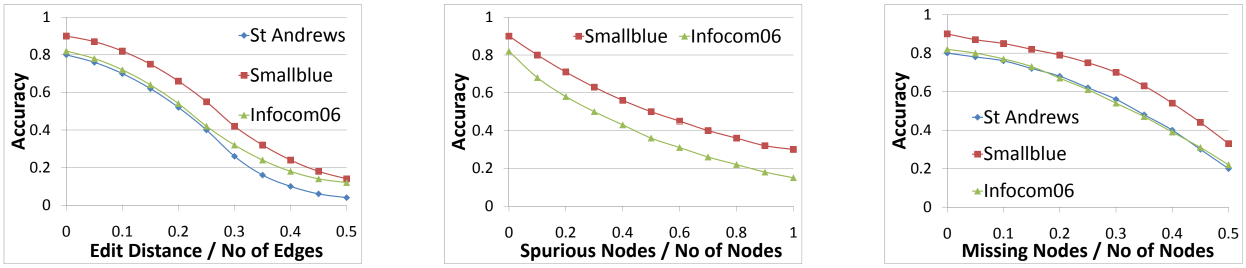

Figure 12: Accuracy with Noisy Social Network

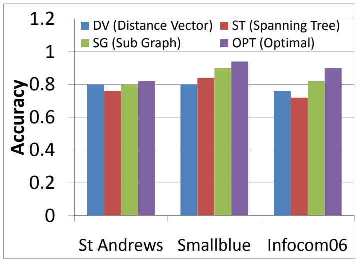

Figure 11: Optimality

metry in which a graph is mapped onto itself while preserving edge−vertex connectivity. Formally, an automorphism of a graph $G = (V, E)$ is a permutation σ of the vertex set V, such that the pair of vertices (u, v) form an edge if and only if the pair $(\sigma(u), \sigma(v))$ also form an edge. It is easy to see that no graph de-anonymization algorithm will be able to distinguish between such pairs of vertices (u, v). It may possible to conclude that $(u, v) \in \{u', v'\}$ (i.e., both the mappings $\{u = u'$ and $v = v'\}$ and $\{u = v'$ and $v = u'\}$ are equally likely) but the exact mapping between $\{u, v\}$ and $\{u', v'\}$ may be indeterminate.

For example, if the graph G is completely connected then the number of automorphisms is $|V|!$, i.e., any permutation of vertex labels results in an isomorphic graph. Similarly, a graph that has no edges also has $|V|!$ automorphisms. Hence, such graphs are completely resilient to graph de-anonymization. Let us consider another example wherein the graph G has a star topology, wherein one vertex v_0 has degree n and all the other vertices $\{v_1, \cdots v_n\}$ have exactly one edge to v_0. In such a graph one can determine the mapping for node v_0, however, any permutations on vertex labels $\{v_1, \cdots, v_n\}$ results in an isomorphic graph. Indeed a graph with a star topology has $(|V| - 1)!$ automorphisms.

While graph automorphisms (and its counting version, i.e., determining the number of automorphisms) is a NP-complete problem there are various tools that are very effective in estimating the number of automorphisms for a given graph. For example, Saucy2 [8] has been effective in computing the number of automorphisms in graphs of size ranging from 3K to 5M and number of automorphsisms ranging from $4 - 10^{8000}$ in under 30 minutes. Figure 10 shows the number of graph automorphisms on both the contact graphs C and the social networks S in our datasets. We note that the maximum possible information gain achievable by any graph denonymization algorithm is given by: $\log_2 |V|! - \log_2 max(|aut(C)|, |aut(S)|)$, where $|aut(G)|$ denotes the number of automorphisms of graph G.

We derive an upper bound on accuracy that may be achieved by any de-anonymization algorithm using the number of graph automorphism. In particular, if the social network S has $|aut(S)|$ automorphisms and contact graph C has $|aut(C)|$ automorphisms then the accuracy of any de-anonymization algorithm cannot exceed $min(1 - \frac{\eta_C}{|V_C|}, 1 - \frac{\eta_S}{|V_S|})$, where η_S is the smallest natural number such that $\eta_S! \geq |aut(S)|$ and η_C is the smallest natural number such that $\eta_C! \geq |aut(C)|$.

Figure 11 shows a comparison of our algorithms: DV (landmark based distance vectors), ST (randomized spanning trees), SG (recursive sub-graph matching) and OPT (automorphism bound). Our results show that the recursive sub-graph matching approach consistently outperforms the other approaches. The figure also shows that the nodes in the contact graphs exhibit significant heterogeneity: the automorphism bound on St Andrews, Smallblue and Infocom06 datasets is 82%, 94% and 90% respectively. We note that the recursive sub-graph matching can achieve up to 97.6%, 95.7% and 91.1% of optimality respectively on St Andrews, Smallblue and Infocom06 datasets.

4. EVALUATION: TOLERANCE TO NOISE AND OBFUSCATION

This section presents an evaluation of the efficacy of our algorithms on altered datasets. In particular we will examine the efficacy of our algorithms when: (i) the social network or the contact graph is obfuscated, (ii) a small subset of nodes mappings are known a prior (e.g., insiders reveal their identities or some node mappings are inadvertently leaked), and (iii) examine the efficacy of de-anonymization when stale social networks are used. Our results show that even when about 25% of the social network and the contact graph is intentionally modified (e.g., edges/nodes are added/removed) our approach is effective; further, when a small fraction (5%) of select node mappings (in particular, nodes with low centrality score) are known a priori, then the effectiveness of our approach can exceed 95% (i.e., 95% of nodes are correctly mapped).

4.1 Noisy Social Network

Figure 12 shows the accuracy of node de-anonymization when the social network is obfuscated. We examined three different types of noise that could be added to the social network. First we add/delete edges in the social network − for example, when *edit distance / No of edges* is 0.1 then 5% of randomly selected edges are deleted from the graph, followed by introducing edges between 5% of the ran-

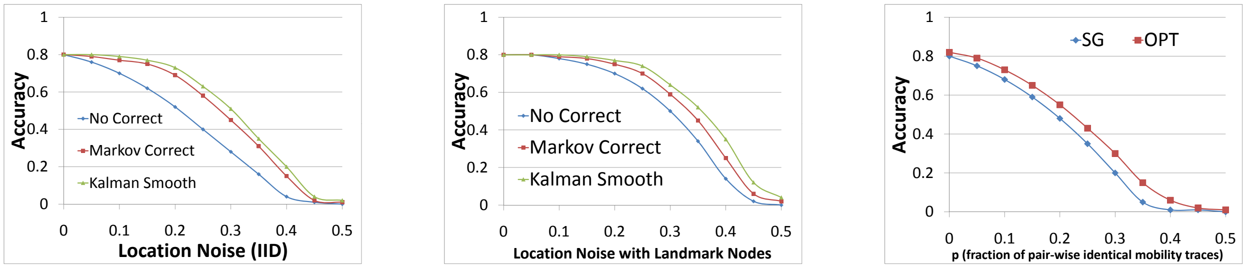

Figure 13: Accuracy with Obfuscated Mobility Traces

domly chosen pairs of nodes. Note that in this case no new nodes are introduced into the social network.

Second we introduce spurious nodes into the social network, that is, users that did not participate in the mobility trace. Note that for both the Smallblue and Infocom06 dataset we have the social network over a superset of users that participated in the mobility trace; hence, we randomly add nodes from the social network (including respective edges to nodes that were already part of the social network). For example, when *Spurious Nodes / No of Nodes* equals 0.1 then 10% of randomly chosen nodes is added to the social network as follows: let V_S denote the set of vertices in the current social network; let $ngh(V_S)$ denote the set of neighbors of vertices in V_S; we pick one vertex at random from the set $ngh(V_S) \setminus V_S$ and add it to the social network; the process is repeated until the required number of nodes are added to the social network. In this case, the size of the resulting social network has 10% more nodes than the contact graph.

Third we randomly remove nodes (and all incident edges) from the social network. For example, when *Missing Nodes / No of Nodes* equals 0.1 then 10% of randomly chosen nodes (and respective edges) is removed from the social network. In this case, the resulting social network is 10% fewer nodes than the contact graph.

In all of Figure 12 we used our *recursive sub-graph matching* algorithm since it performed the best under normal circumstances. The x-axis in the figures quantifies the extent of obfuscation and the y-axis shows the accuracy of our algorithm. We note that in general the efficacy of our algorithm degrades gracefully with the extent of obfuscation. Compared to the other modifications, adding spurious nodes into social network has the most deleterious effect on deanonymization. Intuitively, adding spurious nodes increases the number of possible node mappings by reducing the number of discriminating features.

4.2 Noisy Contact Graph

Figure 13 shows the accuracy of node de-anonymization when the mobility trace is obfuscated. In this experiment we use the location information available from the St Andrews trace. We note that in both the Smallblue and Infocom06 dataset we only have the contacts. We examine the efficacy of our recursive sub-graph matching algorithm as we add more noise to the mobility trace – in our experiments we add IID (independent and identical distributed) noise to the location of each user each point in time. As shown in past work, one can use physical limitations on the speed at which a user may move and aggregate *mobility models* to de-obfuscate the mobility trace. In particular, we use the mobility trace to construct a Markovian mobility model built over all users: $Pr(l_{t+1}|l_t)$, the probability that a user may be location l_{t+1} at time $t + 1$ given that the user was at location l_t at time t.

We use the Markovian mobility model (built over all users) to enrich per-user mobility traces. In particular, we used two techniques to refine the obfuscated mobility trace: (i) using Viterbi decoding [31] to deduce the location of user u at time t (this algorithm is quadratic in the number of states = number of location identifiers) and (ii) using Kalman filtering [31] for both backward and forward smoothing to deduce the location of user u at time t (this algorithm is cubic in the number of states = number of location identifiers). We note that these both Viterbi decoding and Kalman smoothing is applied as a pre-processing to enrich the mobility trace – the enriched mobility trace is then used as input by the recursive subgraph matching algorithm.

Figure 13 shows the effectiveness of adding location noise to: (i) all nodes in the mobility trace and (ii) to only landmark nodes in the mobility trace. We note that using more sophisticated smoothing and state estimation algorithms (e.g., Kalman filter) enhances the efficacy of de-anonymization (at a added computational cost). We also note that adding noise to the mobility traces of landmark nodes is not quite effective; this is because we detect landmark nodes that are *outliers* with respect to node centrality score. In general the centrality score of landmark nodes are significantly higher than the remaining nodes; hence, even with added location noise the centrality score of landmark nodes tend be outliers. For example, consider a star topology contact graph, wherein all nodes $\{v_1, v_2, \cdots, v_n\}$ are in contact with node v_0 and there is no contact between two nodes v_i and v_j such that $1 \leq i < j \leq n$. Even with added location noise we see that it is easy to identify node v_0.

Figure 13 also shows the efficacy of our algorithm when p% of user mobility traces are identical, that is, we randomly select p% nodes and for each selected node v we select a random node v' and set the mobility trace of v to be identical to that of v'. Doing so makes the nodes v and v' automorphic in the contact graph, thereby, decreasing the effectiveness of de-anonymization. We note that this approach is more effective in lowering the efficacy of our algorithm than adding IID location noise to user mobility traces. Note that in this approach to location obfuscation the use of Viterbi decoding or Kalman filter does not enhance the effectiveness of de-anonymization.

4.3 Known Node Mappings

In certain cases one may a priori know the mappings between a small subset of nodes in the social network and the contact graph. This could be due to information that is inadvertently leaked or due to insiders (who participated in the mobility trace) that reveal their mapping information. Figure 14 shows the increase in effectiveness of de-anonymization when more node mappings are revealed. We simply add known node mappings in addition to high centrality node mappings as a seed mapping and uses recursive sub-graph

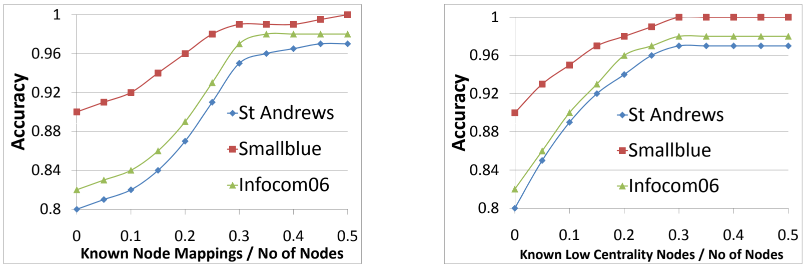

Figure 14: Accuracy with Known Node Mappings

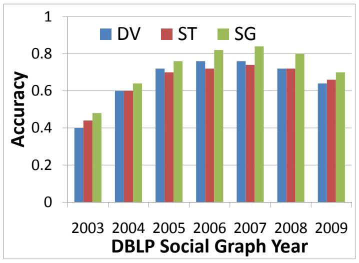

Figure 15: Effectiveness of de-anonymization using DBLP co-authorship graphs from various years

matching algorithm to derive the node mappings for other nodes in the contact graph. For example, when *Known Node Mappings / No of Nodes* is 0.1 then 10% of node mappings are assumed to be known a priori. We observe that given about 30% random node mappings the accuracy of de-anonymization exceeds 95%.

We remark that knowing the node mappings for high centrality nodes is not quite useful for de-anonymization since our algorithm can detect such mappings with high fidelity. On the other hand, the figure shows the effectiveness of de-anonymization when low centrality nodes are revealed (these are nodes that are hard to de-anonymize).

In the next experiment we sort nodes in ascending order of their centrality score. In Figure 14, when *Known Low Centrality Nodes / No of Nodes* equals 0.1 then the mappings of 10% of nodes that have the least centrality score are assumed to be known a priori. We observe that given 10% random node mappings in the Infocom06 dataset the de-anonymization algorithm achieves an accuracy of 83%, while given the same number of node mappings for low centrality nodes achieves an accuracy of 90% (see Figure 14).

4.4 Which Social Network to Use?

Figure 15 shows the effectiveness of de-anonymization when we use different social networks. In particular, for the Infocom06 dataset we constructed social networks (from DBLP publication database) based on co-authorship information from year 2003, 2004, $\cdots$, 2009 (note that Infocom06 dataset is a mobility trace collected from the Infocom conference conducted in 2006). Figure 15 shows that the effectiveness of de-anonymization initially increases as we approach 2006-07 and then decreases. However, we observed that the de-anonymization is most effective using the 2007 co-authorship social network. We conjecture that this is because authors who met at the 2006 conference collaborated and co-authored papers that were subsequently published in 2007. We could in part verify this conjecture by measuring the number of co-authored papers in 2006 and 2007 respectively, by authors who met frequently during the 2006 conference — indeed our dataset shows a 12% increase in the number of such co-authored papers. Hence, the effectiveness of 2007 social network (over the 2006 social network) can be explained by its stronger causal relationship with the contact graph in 2006. We remark that this observation serves as a measure to quantify the effectiveness of conferences in increasing collaborative research amongst authors.

5. RELATED WORK

Location privacy (as applied to mobile users) requires that it be hard to track the location of a user given a mobility trace. In particular several authors have examined the predictability and uniqueness of user location traces using diverse tools; for a survey on past work we refer the readers to [19]. For example, 802.11 user fingerprinting [26] attempts to identify a user using *implicit identifiers* such as IP addresses or the service set identifier (SSID) being actively searched by a user's device; others have suggested RF (Radio Frontend) fingerprinting [5] to uniquely identifier a user's device; others have proposed the use of triangulation (e.g., based on received signal strength from multiple vantage points) to further improve the precision of a user's location [17]; others have suggested that a user be fingerprinted using a historical set of locations visited by that user (e.g., a per-user Markovian mobility model as discussed earlier in Section 1); [20] proposes a framework for recognizing mobile users' activities based on the places they visit and also the temporal patterns of their visit.

More recently, Shokri et al. [30] proposed a solution to quantify location privacy with the goal of providing a unified framework that can be used to evaluate various location obfuscation mechanisms. Their paper presents solutions to quantify location privacy given an obfuscated mobility trace and the Markovian mobility model. They show that the effectiveness of an anonymized mobility trace in protecting location privacy not only depends upon the extent of obfuscation but also the fidelity of the auxiliary information. However, their location privacy metrics only apply to auxiliary information of the type per-user Markovian mobility model.

Several authors have explored the use of auxiliary data (sometimes referred to as *side channel* information) to break privacy. A generic template for violating privacy using auxiliary information is often represented as follows [24]: *anonymized data + auxiliary information = de-anonymized data*. Side channels in the form of timing analysis [10] and power analysis [18] have been extensively studied in literature. More recently, authors have used side-channel information (e.g., zipcode, age and sex of users) to de-anonymize the Netflix Prize dataset [24].

The closest related work is [23] that proposes using graph deanonymization for social networks. Their approach in principle is similar to our recursive sub-graph matching approach. However, our work presents various key solutions over prior work: (i) using node centrality to identify landmark nodes and bootstrap deanonymization, (ii) reductions to weighted graph matching and tree edit distance problem, (iii) dynamic CSP formulation can be viewed as a alternate formulation of the approach presented in [23], and (iv) lower bounds based on automorphism. Finally, to the best of our knowledge, this paper presents the first attempt to leverage social networks as a side-channel to de-anonymize user mobility traces.

6. SUMMARY

In this paper we explored an alternate source of auxiliary information − inter-user correlations which can be often inferred from publicly available social networks to de-anonymize mobility traces. A vast majority of past work developed detailed *per-user models* (e.g., a per-user Markovian mobility model) and used such models to identify the most probable user that could have generated an anonymized trace. In contrast, this paper studied the use of *inter-user correlation models* to address this problem. In particular, we exploited structural similarities between two sources of inter-user correlations (the contact graph and the social network) and developed techniques to leverage such structural similarities to deduce mapping between nodes in the contact graph with that in the social network, thereby de-anonymizing the contact graph (and thus the underlying mobility trace). We validated our hypothesis using three real world datasets and showed that the proposed approach achieves over 80% accuracy, while incurring no more than a few minutes of computational cost in de-anonymizing these mobility traces.

Acknowledgements

Research was sponsored by US Army Research laboratory and the UK Ministry of Defence and was accomplished under Agreement Number W911NF-06-3-0001. The views and conclusions contained in this document are those of the authors and should not be interpreted as representing the official policies, either expressed or implied, of the US Army Research Laboratory, the U.S. Government, the UK Ministry of Defense, or the UK Government. The US and UK Governments are authorized to reproduce and distribute reprints for Government purposes notwithstanding any copyright notation hereon.

7. REFERENCES

[1] Smallblue. http://domino.research.ibm.com/comm/research_projects.nsf/ pages/smallblue.index.html.

[2] Please rob me. http://pleaserobme.com/, 2012.

[3] A. Biem, E. Bouillet, H. Feng, A. Ranganathan, A. Riabov, O. Verscheure, H. Koutsopoulos, and C. Moran. Ibm infosphere streams for scalable, real-time intelligent transportation services. In *Proceedings of the 2010 international conference on Management of data*, SIGMOD '10, pages 1093–1104, 2010.

[4] G. Bigwood, D. Rehunathan, M. Bateman, T. Henderson, and S. Bhatti. CRAWDAD data set st_andrews/sassy (v. 2011-06-03). Downloaded from http://crawdad.cs.dartmouth.edu/st_andrews/sassy, June 2011.

[5] A. Cohen. Rf fingerprinting pinpoints location. http://www.networkworld.com/news/tech/2004/101104techupdate.html.

[6] W. J. Cook, W. H. Cunningham, W. R. Pulleybank, and A. Schrijver. *Combinatorial Optimization*. Wiley-Interscience, 1997.

[7] P. Crucitti, V. Latora, and S. Porta. Centrality measures in spatial networks of urban streets. In *Physical Review E: Statistical, Non-Linear and Soft Matter Physics*, 2006.

[8] P. T. Darga, H. Katebi, M. Liffiton, I. Markov, and K. Sakallah. Saucy2: Fast symmetry discovery. http://vlsicad.eecs.umich.edu/BK/SAUCY/, 2008.

[9] DBLP. DBLP Bibiography. http://www.informatik.uni-trier.de/ ley/db/.

[10] R. Dingledine, N. Mathewson, and P. Syverson. Tor: The second generation onion router. In *13th USENIX Security Symposium*, 2000.

[11] R. K. Ganti, N. Pham, H. Ahmadi, S. Nangia, and T. Abdelzaher. Greengps: A participatory sensing fuel-efficient maps application. In *In Proc. of Conference on Mobile Systems, Applications, and Services, MobiSys*, pages 151–164, 2010.

[12] W. Gao, A. Iyengar, M. Srivatsa, and G. Cao. Supporting cooperative caching in disruption tolerant networks. In *IEEE Intl Conference on Distributed Computing Systems (ICDCS)*, 2011.

[13] M. Gonzalez, C. Hidalgo, and A.-L. Barbasi. Understanding individual human mobility patterns. *Nature*, 453:779–782, 2008.

[14] J. M. Harris, J. L. Hirst, and M. J. Mossinghoff. *Combinatorics and Graph Theory*. Springer Mathemathics, 2008.

[15] B. Hull et al. Cartel: a distributed mobile sensor computing system. In *Proc. of SenSys*, pages 125–138, 2006.

[16] IBM ILOG Solver. Constraint programming. http://www-01.ibm.com/software/integration/optimization/cplex-cp-optimizer/.

[17] T. Jiang, H. J. Wang, and Y.-C. Hu. Preserving location privacy in wireless lans. In *MobiSys*, 2005.

[18] P. Kocher, J. Jaffe, and B. Jun. Differential power analysis. In *Advances in Cryptology (Crypto)*, 1999.

[19] J. Krumm. A survey of computational location privacy. In *Personal Ubiquitous Computing, 13(6): 391-399*, 2009.

[20] L. Liao, D. J. Patterson, D. Fox, and H. Kautz. Learning and inferring transportation routines. In *Artificial Intelligence 171:311Ű331*, 2007.

[21] H. Lu, W. Pan, N. Lane, T. Choudhry, and A. Campbell. Soundsense: Scalable sound sensing for people-centric applications on mobile phones. In *In Proc. of ACM MobiSys*, pages 165–178, 2009.

[22] I. Miguel. *Dynamic Flexible Constraint Satisfaction and its Application to AI Planning*. Springer, 2003.

[23] A. Narayanan and V. Shamatikov. De-anonymizing social networks. In *IEEE Security and Privacy Symposium*, 2009.

[24] A. Narayanan and V. Shmatikov. De-anonymizing social networks. In *IEEE Symposium on Security and Privacy*, 2009.

[25] T. Opsahl, F. Agneessens, and J. Skvoretz. Node centrality in weighted networks: Generalizing degree and shortest paths. In *Social Networks*, 2010.

[26] J. Pang, B. Greenstein, R. Gummadi, S. Seshan, and D. Wetherall. 802.11 user fingerprinting. In *ACM MobiCom*, 2007.

[27] S. M. Ross. *Introduction to probability models*. Academic Press, 2006.

[28] J. Scott, R. Gass, J. Crowcroft, P. Hui, C. Diot, and A. Chaintreau. CRAWDAD data set cambridge/haggle (v. 2009-05-29). Downloaded from http://crawdad.cs.dartmouth.edu/cambridge/haggle, May 2009.

[29] S. M. Selkow. The tree-to-tree editing problem. In *Inform. Process Lett., 6(6):184Ű186*, 1977.

[30] R. Shokri, G. Theodorakopoulos, J.-Y. Boudec, and J.-P. Hubaux. Quantifying location privacy. In *IEEE Symposium on Security and Privacy*, 2011.

[31] R. F. Stengel. *Optimal Control and Estimation*. Dover Publications, 1994.

[32] A. Thiagarajan, J. Biagioni, T. Gerlich, and J. Eriksson. Cooperative transit tracking using smart-phones. In *In Proc. of Conference on Embedded Networked Systems, SenSys*, pages 85–98, 2010.